ESRF	**Experiment title:** Diffraction studies of ferroelectric thin films under non-ambient conditions	**Experiment number**: 01-02-790
Beamline: BM01-A	**Date of experiment**: from: 05.03.08 08:00 to: 11.03.08 08:00	**Date of report**: 15.10.08
Shifts: 18	**Local contact(s)**: Dmitry Chernyshov	*Received at ESRF:*

Names and affiliations of applicants (* indicates experimentalists):

F. Mo*[a], J.A. Beukes[a], T. Tybell*[b]

In addition these experimentalists Dag W. Breiby[a], Lasse S. Thoresen[a]

[a] Dept. of Physics, Norwegian Univ. of Science and Technology, N-7491 Trondheim, NORWAY

[b] Dept. of Electronics and Telecommunications, Norwegian Univ. of Science and Technology, N-7491 Trondheim, NORWAY

Overview

Periodic domains arise in ferroelectric materials as a compromise in energy associated with various external forces such as depolarizing field, substrate-induced strain and applied electric field. The occurence of domains, their topologies and dynamic behaviour in response to an external electric field are issues of crucial importance for the design and application of these materials in electromechanical and optoelectronic devices.
The coercive field E_c required to reverse the polarization and create a monodomain state increases with decreasing film thickness d as $E_c(d) \propto d^{-2/3}$. For a 100 nm film of $PbTiO_3$ the local coercive field is of the order 200 kV/cm. We have studied epitaxial films of varying d, both under zero field and under a weak field $E << E_c$ in order to investigate as a function of d, 1) domain size and orientation and in-plane strain, and 2) the impact of a weak field on the domain structures, and to what extent the effects are switched on and off with the field. The diffuse scattered intensity near the Bragg reflections gives information both on the average domain periodicity and orientation.

Experimental

Our samples were epitaxial films of $PbTiO_3$ (PTO) deposited by RF magnetron sputtering onto (001) oriented insulating $SrTiO_3$ (STO) single crystal plates of dimension $a \times a \times 0.5$ mm, a = 5–7 mm. The nearly perfect lattice match between cubic STO and the *ab*-plane of tetragonal PTO ensures that the polar *c*-axis of PTO will be well aligned in the growth direction of the film, favouring the formation of *c*-oriented domains. PTO films of thickness 50, 12 and 6 unit cells (uc), corresponding to $d \sim 207$, 49 and 24.5 Å, respectively, were studied by SR X-ray scattering, using a specially designed sample holder for applying an electric field of 4 kV/cm along the polar axis [1]. Several reflections 0 0 l and h 0 l and the associated diffuse scattering were examined without field, under field and again with the field switched off, by scans in ω with step width 0.025° over a range of 3°. Scattered intensities were recorded using a CCD detector with pixel size 60.3 μm placed orthogonal to the X-ray beam at a distance of 360 mm from the sample. For most scans data were binned 2x2 giving an angular resolution ~ 0.02°. Imaging with an area detector is vastly superior to linear *Q*-scans with a point detector for a complete survey of reciprocal space. Rectilinear reconstructions of reciprocal space were done with the CrysAlis software (Oxford Diffraction) and 3D visualization

with new locally developed software allowing fine slicing in a selected rational direction for the subsequent construction of 3D images of the diffuse satellite intensities. The wavelength of the radiation, 0.9697 Å, was selected to avoid fluorescence from the heavy elements of the sample.

Results and brief discussion

The 50 uc film

Various representations of reflection 1 0 3 for the 50 uc film are shown in Fig. 1, 2 and 3 (Attachment). In Figs. (*a*) the film Bragg (central part) and the substrate Bragg (top) reflections are connected by the Bragg truncation rod. The diffuse scattering relaying the domain structure is seen near the film Bragg reflection. The cross-section of the truncation rod is elongated along a^* forming a bridge to the surrounding satellite pattern, see Figs. (*b*). The apparent hole in the centre of the latter figures defines the core of the truncation rod where the relative intensity exceeds the level selected for the iso-intensity surface.

Zero field before application of field Most prominent satellite feature: an annular ring with mean diameter $D \sim 0.036$ rec. lattice units (rlu) = $2\Delta h$. The ring is part of a more diffuse disk extending farther out, and is also part of a diffuse, slightly wedge-shaped cylinder about the c^*-axis, presumably reflecting the limited correlation length along this axis. The annular ring is consistent with stripe domains in nearly random in-plane orientation, with period $\Lambda = a/(D/2)/10$ (nm) where $a = 3.905$ Å, giving $\Lambda \sim 22$ nm.

Under applied field 4 kV/cm. The weak field (< 1 % of the estimated E_c) creates a significant redistribution of the diffuse intensity, hence also in domain structure. This is a surprising result. The strong annular ring has vanished. A much weaker ring with $D \sim 0.043$ rlu appears corresponding to a shorter $\Lambda \sim 18$ nm. A large fraction of the diffuse intensity apparently has migrated into the truncation rod as indicated by an increase of about 33 % in the integrated intensity at the position of the film Bragg reflection. This may imply a general increase in domain period with $\Lambda > 52$ nm as measured along b^*. Subsidiarily, the attenuated diffuse intensity outside the truncation rod may be ascribed also to a larger variation in size distribution, which may affect the measurement of D. Inhomogeneity in size is also very likely for the domains contributing to scattering within the truncation rod.

Zero field after field on. There is no obvious sign of reversal to the prefield state. The diffuse intensity is weaker than with field on. It is slightly convex, with a broad maximum around $\Lambda \sim 20$ nm with a preference for stripes to be lined up parallel to b^*. Intensity has continued to migrate into the truncation rod. The intensity at the film Bragg reflection has increased by about 87 % over the value for the unperturbed sample, indicating a continued growth of larger domains. A narrow disk farther up along the truncation rod is reminiscent of the feature seen under field.

The 6 uc film

All scans of reflection 1 0 3 are very similar with field or without. The distribution obtained with zero field after switching off the field is representative for all exposures and is shown in Fig. 4.

The recurrent feature for all exposures is a diffuse cylinder about the Bragg truncation rod. The mean diameter $D \sim 0.078$ rlu corresponds to a domain period $\Lambda \sim 10$ nm of stripes in a random arrangement. The appearance of a cylinder, not a disk or ring, must be attributed to the much shorter correlation length along c^* in this film. The invariant satellite features show that an applied field of 4 kV/cm is below the threshold needed to induce clear changes in the domain size and distribution in this film, in contrast to the film of thickness 50 uc. The coercive field for the 6 uc thick film is a factor ~ 4 larger than for the 50 uc film.

Conclusions

1) We have shown that the domain structure and its evolution under an electric field can be studied by using 3D reconstructions of reciprocal space. A huge and very detailed body of experimental information can be acquired in a relatively short time with a 2D detector, demonstrating its superiority to 1D Q-scans with a point detector.
2) The observed effect of an applied field < 1 % of the estimated E_c on the domain structure in the 50 uc thick film is a surprising result. The development of the diffuse scattering after the the field has been switched off implies that an immediate reversal to the prefield state does not take place.
3) The invariance of the satellite features in the 6 uc thick film suggests that there should be a critical range in d between 6 and 50 uc (critical $E/E_c(d)$) for which a response to the applied field of 4 kV/cm can be detected.

4) The measurements must be repeated, and for the thinnest films with better statistics, to verify the observations. More films with $d > 50$ uc, $d < 6$ uc and intermediate d should be included, which will also enable an estimate of Λ as a function of d. Allowing longer periods of recovery with the field switched off may give information on domain wall kinetics.
5) A new set of slits with the limiting aperture closer to the sample has provided a more precise definition of the beam cross-section and a much improved intensity profile. In the next run the movements of the slit system will be motorized for remote control. We have now also a goniometer head with motorized z-translation which will facilitate remote centering of the sample surface in the diffractometer coordinate system.
6) Future work will include grazing incidence diffraction.

A brief account of this work has been presented at the XXI IUCr Congress in Osaka, 2008 [2].

[1] F. Mo, K. Ramsøskar: A sample cell for diffraction studies with control of temperature, relative humidity and applied electric field. To be submitted to J. Appl. Cryst.

[2] F. Mo, D. Chernyshov, L.S. Thoresen, D.W. Breiby, T. Tybell. *Acta Cryst.* (2008) **A64**, C520-521

Attachment to report on Exper. No. 01-02-790

50 uc thick film

Fig. 1

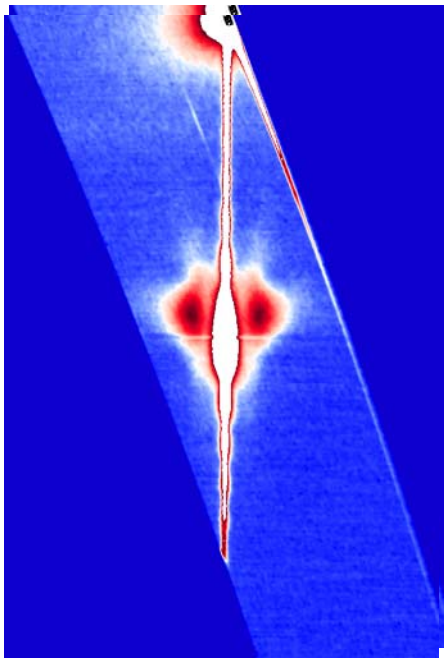

(a)

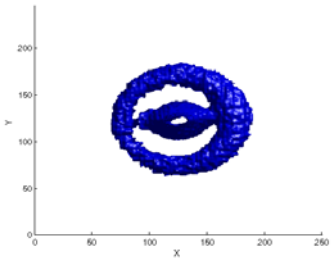

(b)

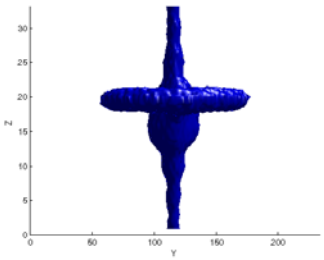

(c)

Fig. 1. No field before field on.

Fig. 2

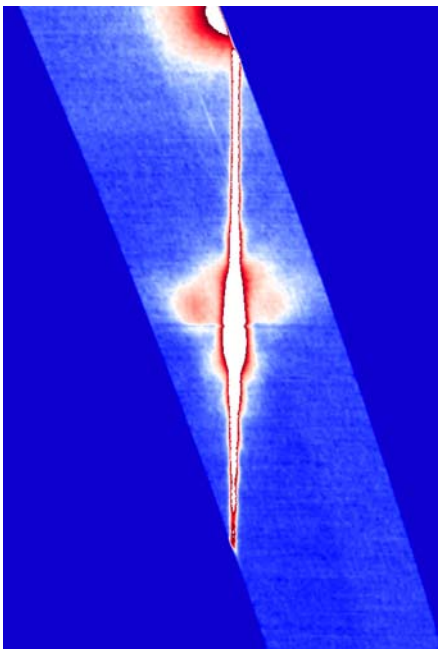

(a)

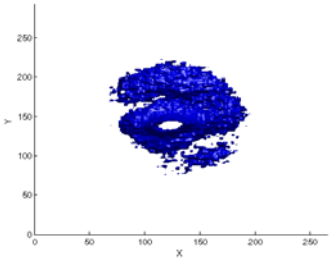

(b)

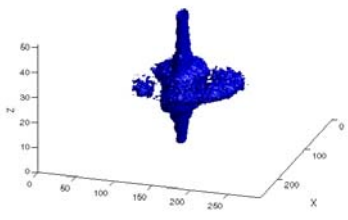

(c)

Fig. 2. Under field.

Fig. 3

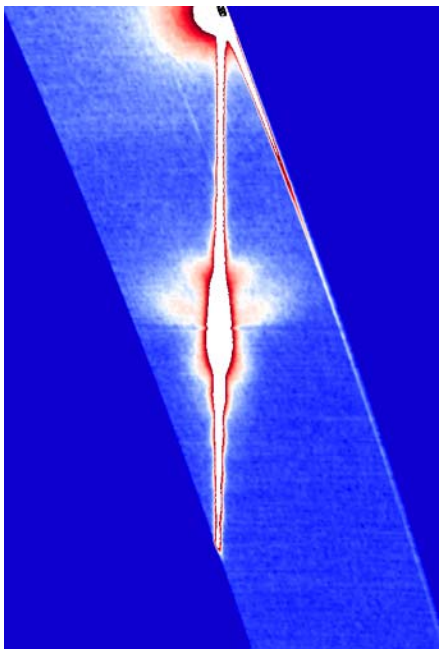

(a)

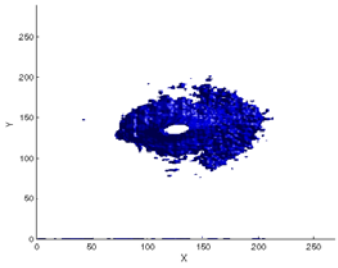

(b)

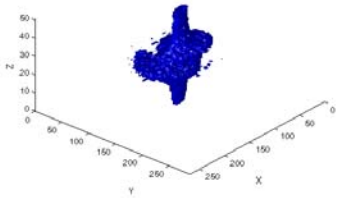

(c)

Fig. 3. No field after switching off field.

Figs. (a): *b*c**-slice through central part of the Bragg intensity. Figs. (b): *a*b** view of 3D reconstructions. Iso-intensity surface of the diffuse scattering, rel. intensity level: ~ 1400 (Fig. 1), ~ 500 (Fig. 2), ~ 450 (Fig. 3). Figs. (c): *b*c** view of the same intensity distribution as in Fig. (b) (Fig. 1); Perspective view of the same intensity distribution as in Fig. (b)) (Figs. 2 and 3)

6 uc thick film

Fig. 4. Exposure with no field ~ 2h after switching off field

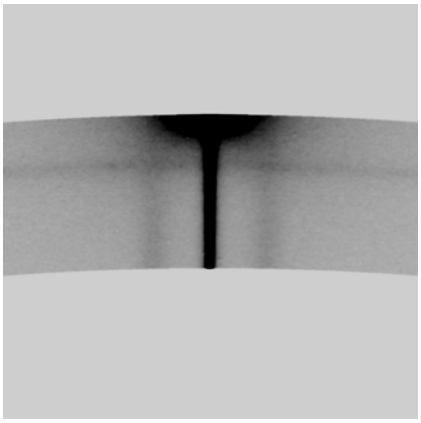

(a)

(a) *b***c**-slice through central part of the Bragg intensity.

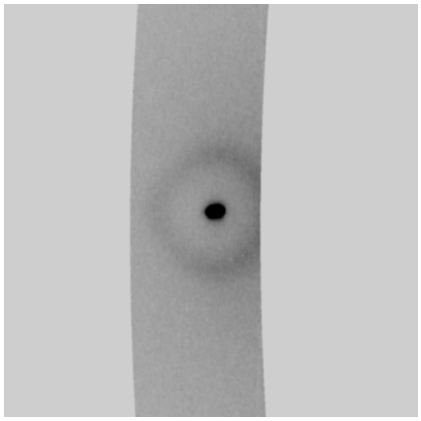

(b)

(b) *a***b**-slice through central part of the Bragg intensity.